Space Potential Measurement of Laser Ablation Plasma for Electrostatic Acceleration

By Ayaka HAMADA,[1)] Kaede YANO,[1)] Takato OGASAWARA,[1)] Hideyuki HORISAWA,[1)] and Haruo SHINDO[2)]

[1)]*Department of Mechanical Engineering, The University of Tokai, Hiratsuka, Japan*
[2)]*Plasma Research Laboratory CO.LTD., Sagamihara, Japan*
(Received June 21st, 2019)

In this study, development of a laser-electrostatic hybrid acceleration thruster was conducted, which is a combination of a laser propulsion system and an electrostatic propulsion system. Since this system can additionally accelerates ions by accelerating laser-ablation plasma by an external electrostatic field, highspeed ions can be generated. In this study, to obtain spatial and temporal plasma parameters for the optimum acceleration, Langmuir probe measurement of laser-ablation plasmas was firstly conducted, where focused Nd:YAG laser pulses were irradiated on a copper target in a vacuum chamber. Temporal changes of spatial distributions of the plasma parameters were obtained. As the results, the maximum electron temperatures varied from 6.4 eV to 1.5 eV at probe positions at 150 mm and 170 mm respectively

Key Words: Diagnostics, Langmuir Probe, Laser Propulsion, Plasma

1. Introduction

Small-sized onboard laser plasma thrusters are under significant development with rapid evolutions of compact but high-power laser systems.[1)~4)] One of the advantages of such laser thrusters is the use of solid-state materials for the propellant. Since any solid material can be used for the propellant, tanks, valves, or piping systems, which are necessary for the thrusters with liquid or gaseous propellant, are not required for the laser propulsion system. Therefore, the laser thruster system can be very simple and compact. Also, significant controllability of thrust is possible by changing the input laser power. In order to further improve the thrust performances and system simplicities of those conventional laser propulsion systems, a preliminary study on a laser-electric hybrid propulsion system was conducted.

2. Electrostatic acceleration by laser induced plasma

Our laser-electric hybrid acceleration system is depicted in Fig. 1. The basic idea of these systems is that a laser-ablation plasma, induced by the laser irradiation on a solid target, is additionally accelerated by an accelerator grid. Because the laser-ablated plasma has the initial velocity of about 10 km/s, specific impulses can be significantly increased with further acceleration of ions by an electrostatic regime. In this case, relating to electrode configuration, plasma density, electrical input-power (voltage and current), etc., acceleration regimes for the laser-ablation plasma can be classified into three types, i.e., i) electrostatic acceleration, ii) electromagnetic acceleration, and iii) electrothermal acceleration. Especially for the laser-ablation plasma, depending on laser conditions such as pulse energy, fluence, etc., plasma density distribution can be widely controlled. Moreover, this can also be increased through additional electric discharges. Therefore, optimizing the electrode configuration for additional electric acceleration, and properly controlling a power source, or voltage and current, adapting to each acceleration mechanism, the propulsion system satisfying all the above acceleration schemes through i) to iii) can be achieved with one thruster configuration. Namely, this system enables a robust conversion between high specific impulse operation and high thrust density operation in regard with mission requirements. Each of two typical types of the acceleration schemes are currently being investigated as described in following subsections.

In this study, to reveal the acceleration mechanism of the laser-electrostatic hybrid thruster, the plasma plume near the ablation target was characterized by the Langmuir probe.

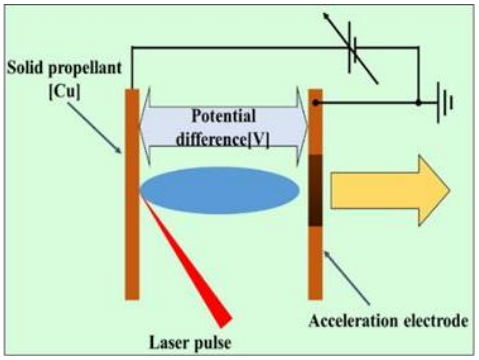

Fig. 1. Schematics of laser ablation thrusters.

3. Experimental apparatus

Figure. 2 shows a schematic of the experimental setup for laser induced plasma diagnostics. A laser beam oscillated by an Nd: YAG laser oscillator (wavelength 1064 nm, pulse energy

174 mJ / pulse, pulse width 5 ns) was introduced into a vacuum chamber after being expanded by a beam expander. At this time, scattered light generated in the laser introducing window was acquired by a photodiode, and this was used as a trigger (an origin of time) of an oscilloscope for recording a time history of a probe output current. The vacuum chamber was maintained at a degree of vacuum of 10^{-3} Pa order by a turbo molecular pump. The laser light introduced into the chamber was reflected by a mirror, focused by a final stage lens, and irradiated on the surface of a solid propellant (oxygen-free copper). At this time, the laser induced plasma generated was diagnosed with a flat single Langmuir probe (size: 5 mm × 5 mm) installed on a uniaxial stage movable on an axis perpendicular to the surface of the propellant from the focusing point. In addition, as shown in the figure, a vector of the probe surface was arranged to the direction (parallel) which parallel the plasma flow. An arbitrary bias voltage was applied to the Langmuir probe, and the time change of the ion / electron current was acquired for each laser pulse. In addition, the probe was mounted on a movable uniaxial stage so that the spatial distribution of plasma could also be diagnosed. In addition, the focusing point on the surface of a propellant was able to move on a movable stage in order to refresh an irradiated surface after each laser pulse irradiation. Further, for comparison, the diagnosis was also performed in the case where the probe surface was facing vertically to the plasma flow (the direction rotated 90 ° from the direction of the probe in the figure).

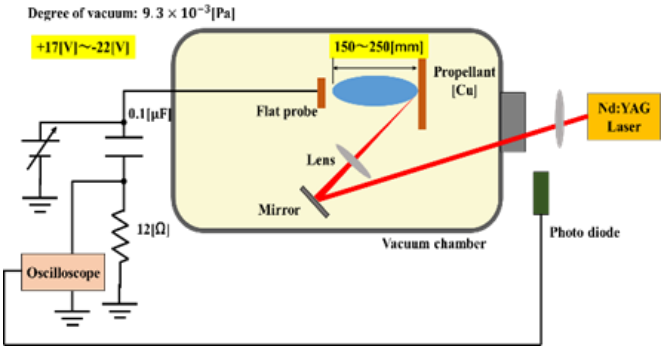

Fig. 2. Experimental Setup of Single Probe Measurement.

4. Results and Discussion

4.1 Probe surface facing parallel to the plasma flow

Figure 3 shows the temporal variation of the probe current (probe position: 150 mm from the surface of the propellant) at each bias voltage when the probe surface is facing parallel to the plasma flow. In this figure, the temporal changes of the probe currents at various bias voltages are displayed in different colors. Generally, in single-probe plasma diagnosis, a relatively steady (equilibrium state) plasma having a characteristic time sufficiently longer than the plasma frequency is targeted. In this case, a change in probe current when the probe bias voltage is continuously changed is measured. On the other hand, the laser induced plasma handled in this research requires relatively high time resolution diagnosis. In this experiment, diagnosis was made according to the following procedure using the fact that there is no big difference in a plasma condition for each laser pulse irradiation, and the reproducibility of the phenomenon is assumed to be high.

Firstly, while the probe bias voltage (arbitrary) at an arbitrary position was fixed, the temporal change of the probe current is acquired with an oscilloscope. The multiple waveforms can be obtained by repeating the measurement with changing the bias voltages, as shown in Fig.3. From the temporal changes of probe currents at various probe voltages, the voltage-current characteristics at arbitrary times can be extracted by slicing the current waveforms at an arbitrary time, and extracting a relationship between the bias voltage and the probe current (Fig. 4). From the voltage-current characteristics, the electron temperature and density at that time can be estimated. By performing this process for all the time targeted, the temporal changes of the plasma parameters were estimated[6]. In this study, the time interval for extracting the voltage-current characteristics was defined as 100 ns, and various probe positions and quantities at each time were estimated. In addition, since the data obtained in this process is very huge, the calculation processing was made more efficient by adopting parallel processing using MATLAB. The electron temperature can be derived by finding the slope of the current-voltage characteristic from the following equation. [6), 8)]

$$\frac{d\ln I_e(V)}{dV} = -\frac{e}{kT_e} \tag{1}$$

Here, e is an elementary charge, k is a Boltzmann constant, and Te is an electron temperature. In the processing using MATLAB, the current-voltage characteristics for the number of time plots (for example, 500) per 100 ns were extracted, and the temporal variation of the electron temperature was calculated. The electron density (Eq. (2)) and Debye length (Eq. (3)) were additionally calculated using the estimated electron temperature and the following formula, and then the temporal variation of the plasma parameters was estimated.

$$N_e = \frac{4I_{e0}}{eSv_e} \tag{2}$$

$$\lambda_e = \sqrt{\frac{\varepsilon_0 kT_e}{e^2 N_e}} \tag{3}$$

Here, I_{e0} is a saturated electron current, S is a surface area of a probe, v_e is an electron thermal velocity, and ε_0 is a dielectric constant of vacuum.

Figure 5 shows a temporal evolution of the electron temperature at each probe position. It was confirmed that the arrival time of the highest temperature of the electron temperature at each probe position tends to be delayed to reach the highest temperature as the probe position moves downstream from the propellant. Also, the value of the maximum temperature decreases with the increase of the propellant-probe distance. On the other hand, the electron

temperature at each probe position after reaching the maximum temperature tends to rise slightly as it gets farther from the propellant.

Figure. 6 shows the temporal change of electron density at each probe position. It was confirmed that the electron density reaches lowest values at the time when the electron temperature peaks at each probe position. In addition, the minimum value of the electron density at each probe position increases as the distance between the propellant and the probe increases, and after reaching the minimum density, the temporal evolution of density (gradient of each waveform) is relaxed as the distance from the propellant.

Figure. 7 shows the time variation of Debye length at each probe position. The change in Debye length with time shows the same tendency as the electron temperature, and the maximum temperature decreases with the increase in the distance between the propellant and the probe, and at the same time there is a delay in the time to reach the maximum value.

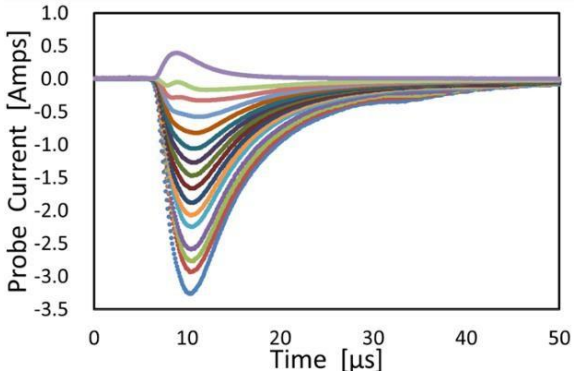

Fig. 3. Temporal Evolution of Probe Currents for Various Probe Biasing Voltage. (Probe in the Parallel to the Plasma)

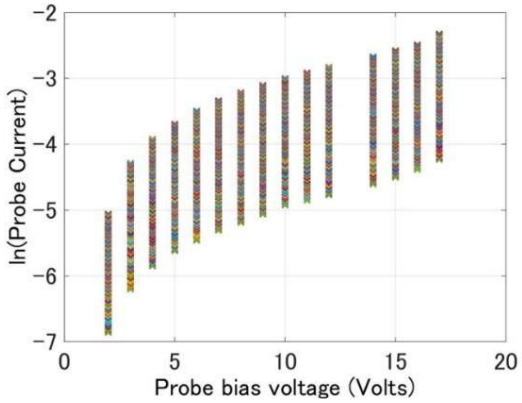

Fig. 4. I-V Characteristics. (Probe in the Parallel to the Plasma)

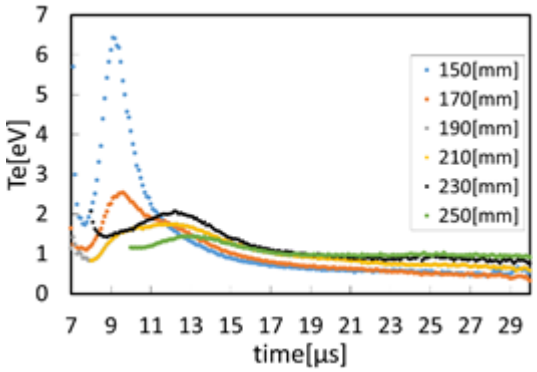

Fig. 5. Temporal Evolution of the Electron Temperature.

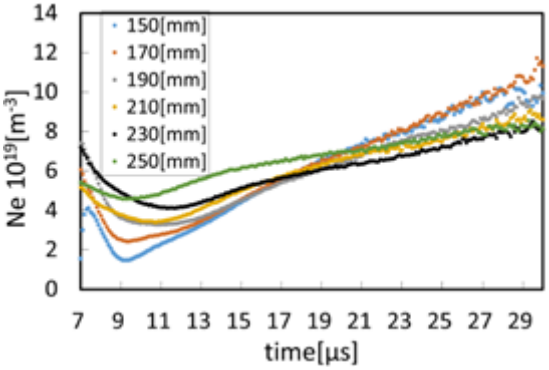

Fig. 6. Temporal Evolution of the Electron Density.

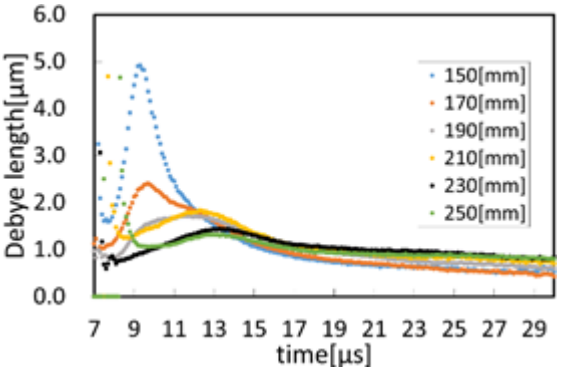

Fig. 7. Temporal Evolution of Debye Length.

4.2 Probe surface perpendicular to the plasma flow

Figure. 8 shows the time variation of the probe current at each bias voltage obtained when the flat plate probe is placed vertically to the plasma flow (probe position 150 mm). The absolute value of the probe current tended to decrease at each time as compared to the case where the probe surface was set parallel to the plasma flow. The V-I curve was extracted from the temporal change of the probe current (Fig. 9). From this figure, the temporal change of the electron temperature calculated as described above is shown in Fig. 10. The peak temperature tends to be lowered by about 4 eV at a position of 150 mm as compared with the case where the probe is placed parallel to the plasma flow. The decrease in electron

temperature in the case of vertical facing is considered to be due to the fact that the projected area to the plasma flow is small and the influx of high energy electrons is small, as can be seen from the decrease of the electron flow.

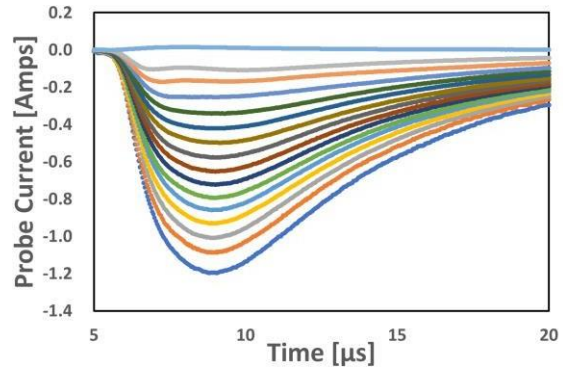

Fig. 8. Temporal Evolution of Probe Currents for Various Probe Bias Voltage. (Probe in the Perpendicular to the Plasma)

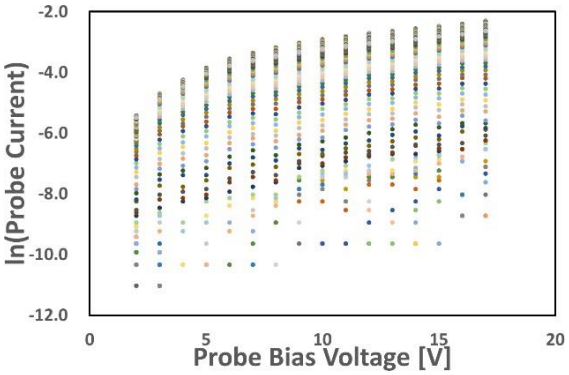

Fig. 9. I-V Characteristics. (Probe in the Perpendicular to the Plasma)

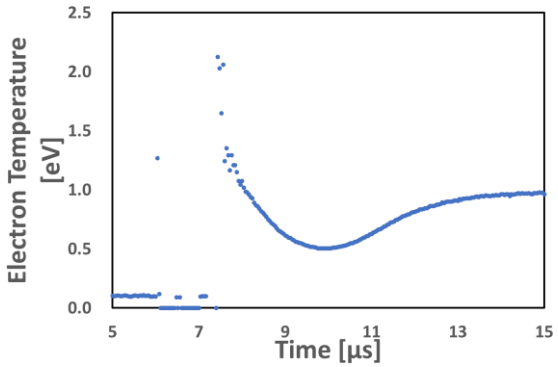

Fig. 10. Temporal Evolution of the Electron Temperature. (Probe in the Perpendicular to the Plasma)

From these results, for effective electrostatic acceleration of the high energy ion component of the laser ablation plasma, it is desirable to apply an accelerating voltage at an early time, ex. less than 10 μs, at a position relatively close to the propellant.

5. Conclusion

In order to realize the effective ion acceleration in the laser / electrostatic acceleration combined thruster, a single Langmuir probe is used in order to understand the spatial structure and temporal behavior of the laser-induced plasma as a propellant in detail. The diagnosis of the laser-induced plasma was carried out. As a result of measurement, when the probe position was moved away from the propellant (moved from 150 mm to 170 mm), the electron temperature decreased from 6.4 eV (at 0.91 μs) to 1.5 eV (at 1.26 μs). In addition, it was confirmed that the electron density tends to be the lowest at 1.5×10^{-19} m $^{-3}$ (at 0.92 μs) when the electron temperature reaches a peak. In addition, it was found that the electron temperature at 150 mm was about 1/3 the size of that at equilibrium when the flat plate probe was installed vertically to the plasma flow. Moreover, the time change of Debye length showed the same tendency as the electron temperature. The peak value of the Debye length was 4.9 μm (9.3 μs). In the future, we plan to conduct more detailed measurements by increasing the number of measurement points.

References

1) Claude Phipps et al., Review: Laser-Ablation Propulsion, Journal of Propulsion and Power, Vol. **26**, No. 4, 2010, pp.609-637

2) Phipps, C. Luke, j.: Diode laser-driven microthrusters: A new departure for micropropulsion, AIAA J., **40**, 2000, pp.310-318

3) Pakhomov, V.A., Gregory, D.A.: Ablative laser Propulsion: An old concept revisited, AIAA J., 38, 2000, pp.725-727

4) Phipps, C. Luke, R. J., Lippert, T. Hauer, M. Wokaun, A.: Mictopropulsion using a laser ablation jey, A. Journal of Propulsion and Power, 20, 2004, pp.1000-1011

5) Nariaki Uchida, Laser Propulsion, 3.4Laser Plasma Engineering (Environment, Space, Industry), 2005

6) L.Torrisi, et.al., Spatial and Temporal Evolution of Laser-Generated Plasmas Measured Through Langmuir Probe, IEEE TRANSACTIONS ON PLASMA SCIENCE, Vol.**42**, NO.3, 2004

7) C.Phipps et.Al., Review of Laser-Ablation Propulsion, Journal of Propulsion and power Vol.**26**, No.4, 2010

8) Brendan Doggetta et.al, Langmuir probe characterization of laser ablation plasmas, JOURNAL APPLIED PHYSICS 105, 033306(2009)

9) M. Capitelli, U. F. Capitelli, and A. Eletskiid, Non-equilibrium and equilibrium problems in laser-induced plasmas, Spectrochem. Acta Part B, Atomic Spectrosc., Vol.**55**, No.6, Jun. 2000, pp.559-574

10) T. N. Hansen, J. Schou, and J. G. Lunney, Langmuir probe study of plasma expansion in pulsed laser ablation, Applied Physics A: Mater. Sci. Process. **69**, 1999, S601-604

11) B. Toftmann, J. Schou, and J. G. Lunny, Dynamics of the plume produced by nanosecond ultraviolet laser ablation of metals, Phys. Rev. B 67, 104101-1-5, 2003

12) B. Toftmann, J. Schou, T. N. Hansen, and J. G. Lunny, Angular Distribution of Electron Temperatire and Density in a Laser-Ablation Plume, Phys. Rev. Lett. 84 (17). pp.3998-4001, 2000

13) B. Doggett, C. Budtz-Hoergensen, J. G. Lunney, P. Sheerin, M. M. Turner, Behavior of a planar Langmuir probe in a laser ablation plasma, Applied Surface Science 247, pp.134-138, 2005

14) S. A. Irimiciuca, S. Gurluib, G. Bulaic P. Nicad, M. Agopd, C. Focsa, Langmuir probe investigation of transient plasmas generated by femtosecond laser ablation of severa l metals: Influence of the target physical properties on the plume dynamics, Applied Surface Science 417, pp.108-118, 2017

15) E. Woryna, P. Parys, J. Wolowski, and W. Mroz, Corpuscular diagnostics and processing methods applied in investigations of laser-produced plasma as a source of highly ionized ions, Laser Particles Beams, vol.**14**, No.3, pp.293-321, 1996

16) G. P. Davis and R. A. Gottscho, Measurement of spatially resolved gas-phase plasma temperatures by optical emission and laser induced fluorescence spectroscopy, J. Appl. Phys., Vol.**54**, No.6, 1983, pp.3080-3086
17) D. C. Carroll, P. Brummitt, D. Neely, F. Lindau, O. Lundh, C. G. Wahlstrom, et al., A bodified Thomson parabola spectrometer for high resolution multi-MeV ion measurements-Application to laser-driven ion acceleration, Nucl. Instrum. Methods Phys. Res. A, Accel., Spectrometers, Detectors Assoc. Equip., Vol.**620**, No.1, 2010, pp.23-27
18) F. Caridi, L. Torrisi, D. Margarone, and A. Borrielli, Evidence of plasmon resonances of nickel particles deposited by pulsed laser ablation, Radiation Effects Defects Solids, Incorporating Plasma Sci. Plasma Technol., Vol.**163**, 2008, pp.357-364
19) R. L. Merlino, Understanding LAngumir probe current-voltage characteristics, Amer. J. Phys., Vol.**75**, No.12, 2007, pp. 1078-1085